Optimal cover designs for outdoor units of air conditioners: A pathway to alleviate the hidden energy burden in Asian megacities

Jiyuan Wu,[1,6] Hailu Wei,[1,2,6] Fengmin Su,[1] Tianzhen Hong,[3] Yuwen Deng,[1] Xiangfeng Li,[1] Qinran Hu,[4,*] and Wei Wang[1,5,*]

*Correspondence: qhu@seu.edu.cn(Q. H.); weiwang@seu.edu.cn(W. W.)

Received: August 19, 2025; Accepted: December 9, 2025; Published Online: January 15, 2026; https://doi.org/10.59717/j.xinn-energy.2026.100136

GRAPHICAL ABSTRACT

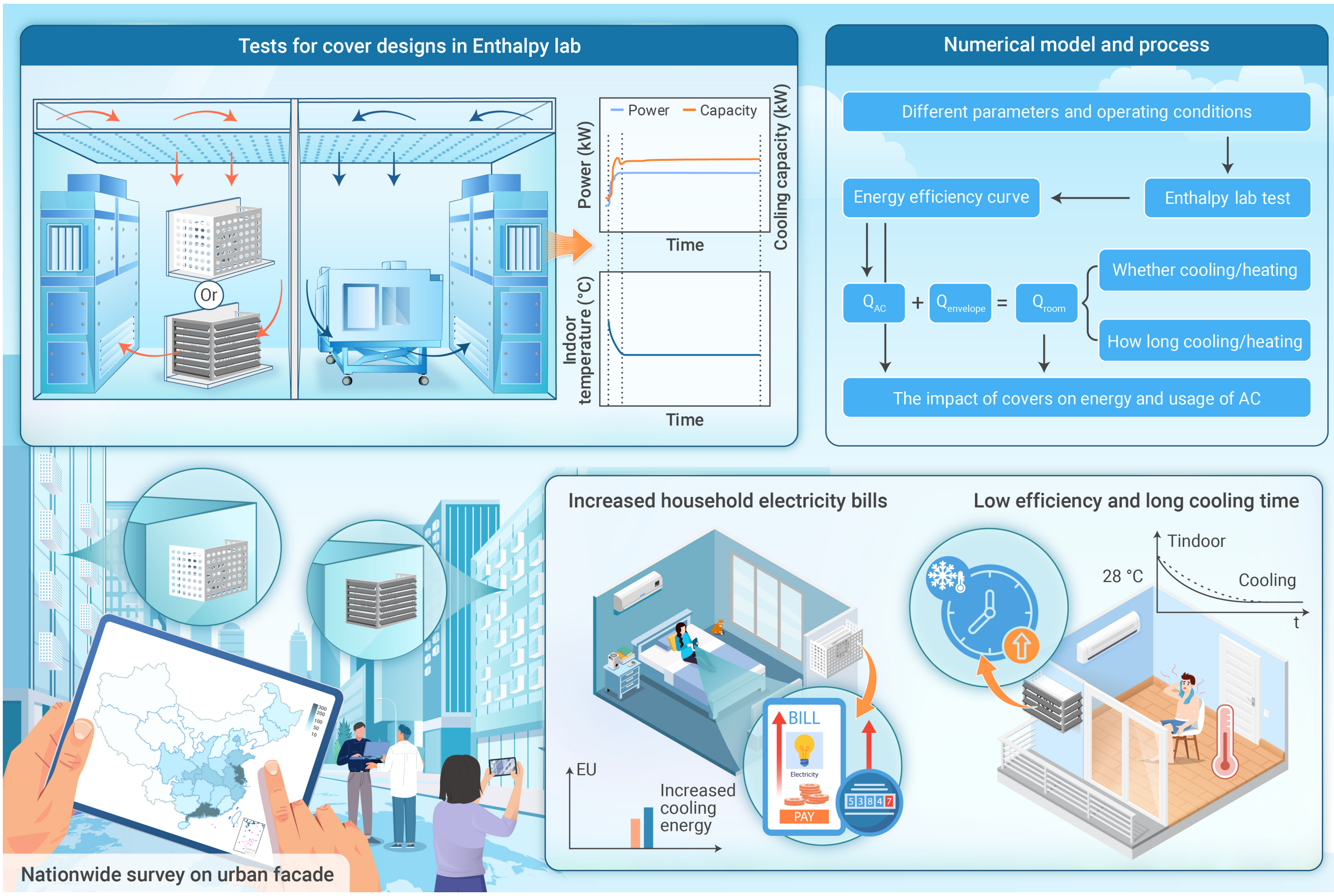

PUBLIC SUMMARY

- Aesthetic AC façade covers can cut cooling efficiency by up to 34% and raise cooling energy use significantly.
- Fully enclosed covers increase building cooling demand by 11.4 kWh/m^2 on average, peaking over 26 kWh/m^2.
- AC operation time is greatly extended by covers, especially during extreme heat events.
- Optimized louver (60°/80°) and orifice (30%/40%) designs nearly eliminate energy penalties.
- Integrating optimized cover designs into façade standards can balance urban aesthetics and energy sustainability.

Optimal cover designs for outdoor units of air conditioners: A pathway to alleviate the hidden energy burden in Asian megacities

Jiyuan Wu,[1,6] Hailu Wei,[1,2,6] Fengmin Su,[1] Tianzhen Hong,[3] Yuwen Deng,[1] Xiangfeng Li,[1] Qinran Hu,[4,*] and Wei Wang[1,5,*]
[1]School of Architecture, Southeast University, Nanjing 210096, China
[2]Department of Building Environment and Energy Engineering, The Hong Kong Polytechnic University, Hong Kong SAR, China
[3]Building Technology and Urban Systems Division, Lawrence Berkeley National Laboratory, Berkeley 94720, USA
[4]School of Electrical Engineering, Southeast University, Nanjing 210096, China
[5]Key Laboratory of Urban and Architectural Heritage Conservation, Ministry of Education, Nanjing 210096, China
[6]These authors contribute to this work equally
*Correspondence: qhu@seu.edu.cn(Q. H.); weiwang@seu.edu.cn(W. W.)

Received: August 19, 2025; Accepted: December 9, 2025; Published Online: January 15, 2026; https://doi.org/10.59717/j.xinn-energy.2026.100136

Citation: Wu J., Wei H., Su F., et al. (2026). Optimal cover designs for outdoor units of air conditioners: A pathway to alleviate the hidden energy burden in Asian megacities. *The Innovation Energy* **3**:100136.

Aesthetic façade covers are widely installed across Asian megacities to conceal outdoor air conditioner (AC) units, yet their energy consequences remain poorly quantified amidst rising cooling demands. This study investigates the unsustainable energy burden imposed by these covers and proposes optimized designs to mitigate it. A comprehensive approach combining laboratory experiments, thermodynamic modeling, and building energy simulations was employed to systematically evaluate the impacts of two prevalent cover types across major Asian climate zones. The core of the methodology involved the development and parametric testing of optimized cover designs through adjustments to louver angles and orifice-plate porosities. Fully enclosed covers severely degraded AC performance, reducing cooling efficiency by up to 34% and increasing building cooling energy use by an average of 11.4 kWh/m^2, with peaks exceeding 26 kWh/m^2 in hotter regions. Cooling operation times were significantly extended, notably during extreme heat events. The results demonstrate that optimized covers can virtually eliminate this energy penalty. Louver covers with 60°/80° angles and orifice-plate covers with 30%/40% porosity limited the average increase in cooling energy consumption to a marginal 0.8 kWh/m^2 reduction and 1.3 kWh/m^2 increase, respectively, compared to uncovered units. The findings reveal that unregulated cover use poses a substantial threat to energy security in Asia. Therefore, it is imperative that these optimized structural parameters are integrated into building facade standards and policies, offering a viable pathway to reconcile urban aesthetics with sustainable cooling.

INTRODUCTION

Urban façade enhancement has emerged as a pivotal governance priority in global cities, mediating the dynamic interplay between built environments and ecological systems while defining metropolitan identity.[1] The past decade has seen exponential growth in façade-focused research, encompassing AI-driven facade recognition algorithms,[2] integration of renewable energy systems,[3] chromatic studies,[4] interactions with urban heat island effects,[5,6] and aesthetic optimization in urban design.[7,8] Nevertheless, the pervasive visual intrusion of outdoor air conditioner (AC) units—ubiquitous yet functionally critical elements—remains a persistent challenge.[9-11] Mandated by thermodynamic necessity to occupy building envelopes, these protrusions generate fractal visual chaos across urban scapes, especially in East Asian megacities where hyperdensity collides with escalating cooling demands, notably e.g., China and Japan.[12-14] The demand for air conditioners is escalating dramatically across Asia, driven by rising incomes, urbanization, and a warming climate. By 2018, household AC penetration in Japan had already reached 91%,[15] while Indonesia, China, and India are projected to account for half of global AC demand by 2050.[16] China alone constituted 40% of the world's installed AC units as of 2020,[17] as shown in Figure S1, with widely used from south to north, as shown in Figure 1A. Outdoor AC units require installation on building facades to facilitate heat exchange,[18-20] yet their proliferation often disrupts the visual coherence of urban architectural landscapes.[1] The collision of surging AC demand[21-23] and rapid urbanization[24] has led to widespread visual clutter from exposed outdoor units.[25]

Nations grappling with this issue, including China and Japan, have universally adopted a strategy of covering outdoor units, as shown in Figure 1B. Uniform covers around outdoor units enhance visual consistency across building exteriors—a practice now deeply embedded in urban buildings, as shown in Figure S1. In the United States, lattice enclosures and decorative planters are common solutions, while Asian countries (e.g., China and Japan) widely deploy metal or wooden frameworks to integrate AC units into building façades.[25] Yet, such covers impose hidden energy penalties and can obstruct the release of hot air and cause heat to build up around outdoor units,[26] negatively impacting AC energy efficiency.[27-30] Mechanistically, AC relies on a refrigerant phase-change and compression cycle, with heat exchange between the indoor and outdoor environments.[31] This cycle is facilitated by a compressor, condenser, and evaporator, as shown in Figure 1D, but AC covers obstruct this process and diminish heat exchange capacity. This leads to prolonged operation times, increased energy consumption, creating a critical conflict between urban aesthetics and sustainable cooling, as shown in Figure 1C.

This study aims to systematically investigate this unsustainable energy burden and propose optimized cover designs to mitigate it. We focus on two prevalent cover types: louver and orifice-plate designs, as shown in Figure 1E. Through a comprehensive methodology combining laboratory experiments, thermodynamic modeling, and building energy simulations across major Asian climate zones, we seek to quantify the impacts of cover structural parameters (louver angle and orifice-plate porosity) on AC performance and to identify optimal configurations that minimize the energy penalty while maintaining aesthetic integration.

METHODOLOGY

Experimental Procedure and Analysis. This study employs laboratory testing and statistical analysis to quantify the direct impacts of cover structural parameters on AC energy performance. Key outcomes assessed include cooling/heating capacity, power consumption, and Energy Efficiency Ratio (EER) / Coefficient of Performance (COP) under various cover configurations and ambient conditions. The analysis correlates cover-induced airflow restrictions with changes in inlet/outlet temperatures and system efficiency.

Experiments conducted in an enthalpy difference laboratory compliant with China national standard GB/T 7725-2022 quantified the impact of AC outdoor unit cover structural parameters on energy performance. The facility comprised two environmentally controlled adjacent chambers: an indoor space simulating conditioned buildings and an outdoor chamber replicating ambient conditions, with the latter regulated by an air handler, as shown in Figure 2B. Using air sampling devices, dry-bulb/wet-bulb temperatures and airflow rates at AC supply/return vents were measured to calculate enthalpy differences, thereby deriving cooling/heating capacities. Tested configurations included louver covers with adjustable tilt angles (0°–80°) and orifice-plate covers with porosity ratios (hole-area/total-area) ranging from 0% to 40%, where maximum porosity was constrained by structural integrity limits, as shown in Figure 2A. All covers were mounted at manufacturer-specified distances: 0.15 m front clearance and 0.2 m side clearance from AC units, as shown in Figure 2A. Ambient temperatures spanned 30°C–50°C (cooling

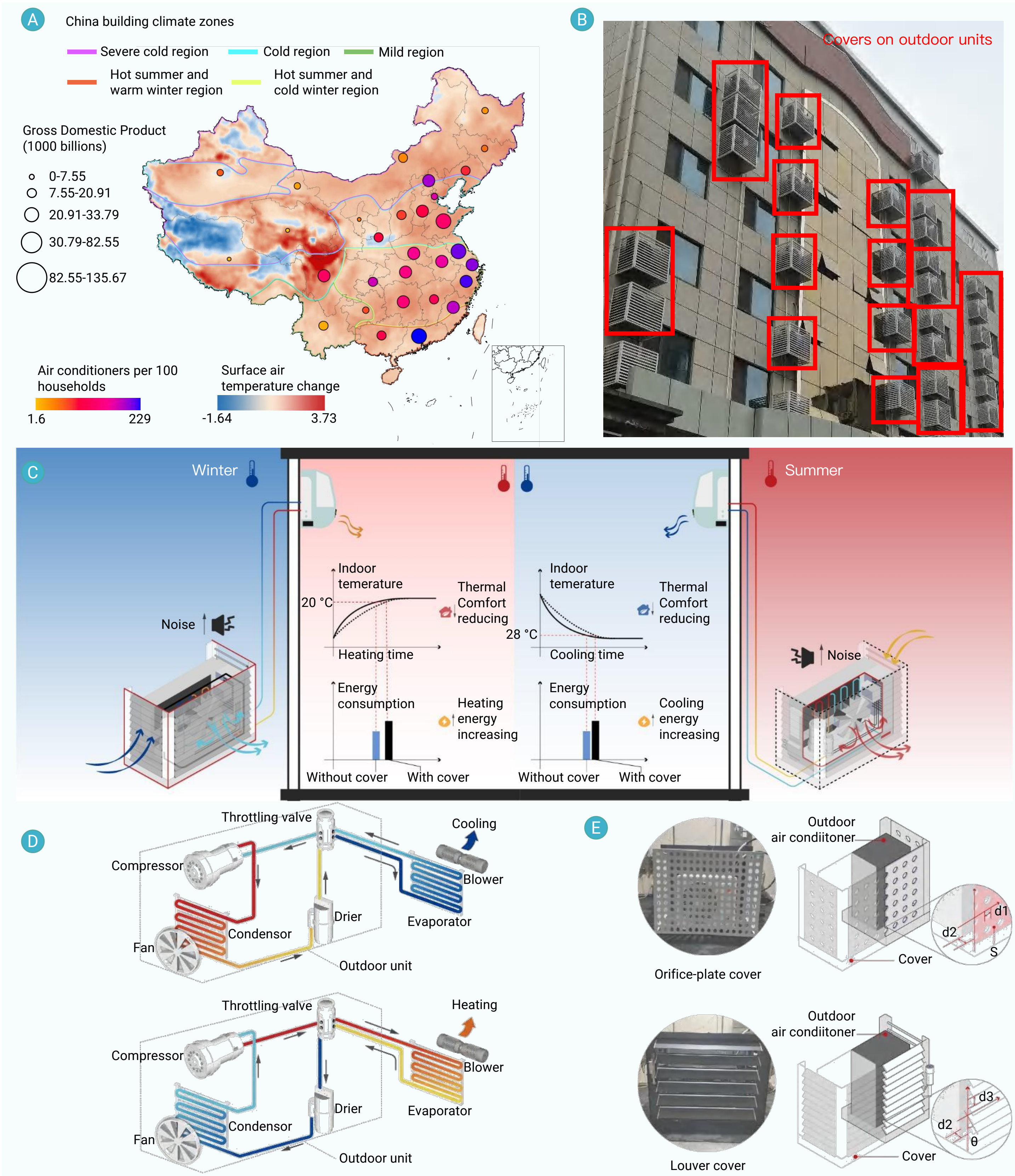

Figure 1. Impacts and key structural parameters of AC Outdoor Unit Covers (A) Map of air conditioner ownership distribution. (B) Photo of covers on outdoor units. (C) Negative impacts of air conditioner outdoor unit covers. (D) Operating principle of AC systems. (E) Key structural parameters of louver and orifice-plate covers.

mode, indoor: 28°C DBT and 19.8°C WBT) and -10°C–10°C (heating mode, indoor: 20°C DBT and 14.8°C WBT) in 4°C increments, as shown in Table S1. This study only considered the influence of outdoor dry-bulb temperature. The relative humidity was fixed at 40.3% (for cooling) and 86.8% (for heating), in accordance with the measurement standard for enthalpy difference laboratory in China's national standard GB/T 7725-2022.

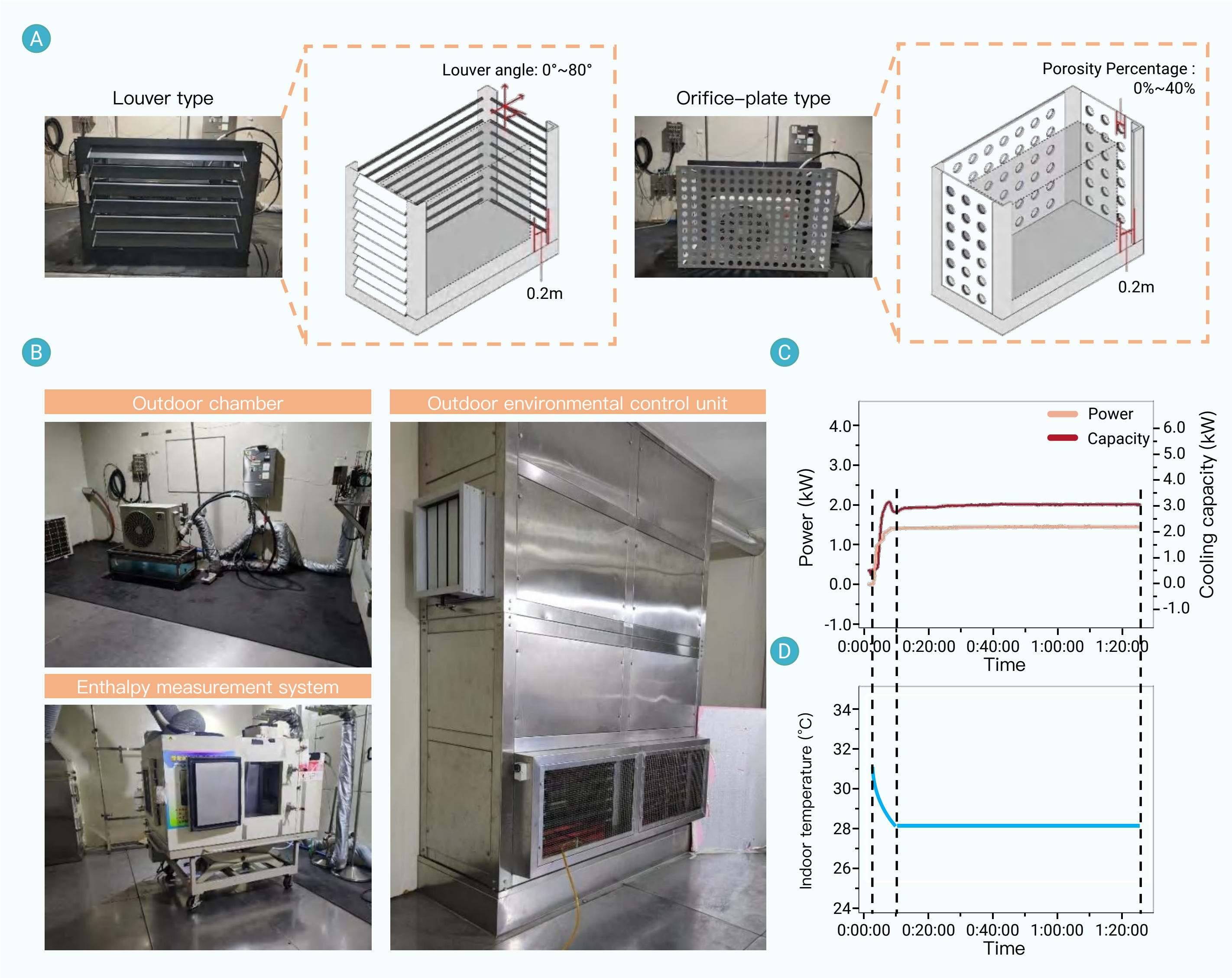

Figure 2. Laboratory and thermodynamic modeling (A) Test article. (B) Enthalpy difference laboratory. (C) Laboratory-measured power and cooling capacity curves. (D) Changes of indoor temperature.

Thermodynamic Modeling and Analysis. This study develops a dynamic thermodynamic model to simulate AC system operation under realistic building loads. The analysis solves energy balance equations using MATLAB to predict transient indoor temperature profiles and system runtime. Outcomes include cooling/heating time required to reach setpoint temperatures under different cover scenarios, linking laboratory performance data to real-world operational behavior.

The energy performance curves of the AC system obtained from laboratory tests reflect only the mechanical performance of the system, as shown in Figure 2C. To accurately represent real-world conditions, these energy performance curves must be integrated with the characteristics of the cooling and heating load. Therefore, this study develops a thermodynamic model to evaluate the AC system's performance under actual operating conditions. Given that the focus is on AC systems obstructed by covers, which are primarily designed for spaces ranging from 15 to 23 m^2, a 20 m^2 building model is constructed for this analysis. The physical attributes of the building and the thermophysical properties of the indoor air are detailed in Table S2.

The thermodynamic model is established based on the performance curves derived from experimental measurements. The operational principle of the AC system is as follows: upon receiving an activation command, the cooling and heating capacities, as well as the power consumption of the AC system, increase according to the laboratory-measured performance curves, as shown in Figure 2D. There are two key scenarios considered:

- In the first scenario, as the capacities increase, the supply air temperature at the return air grille of the indoor unit (which reflects the room temperature) reaches the set point, leading the AC system to cease further capacity increase and enter a stable state.
- In the second scenario, if the cooling or heating capacity reaches the stable value established in the laboratory and the room temperature has not yet reached the set point, the capacity will be maintained at this stable value until the desired temperature is achieved.

For this thermodynamic model, the following assumptions are made: the performance curves of the AC system measured in the laboratory are simplified to assume a direct proportionality between cooling and heating capacity and time from startup to stabilization.

In the summer season, for the first scenario, based on the principle of conservation of energy and neglecting the heat storage in the building envelope, we can derive the following:

$$Q_{AC} = Q_{occ} + Q_{eq} + Q_{envelop} + Q_{air} \quad (1)$$

Here, Q_{AC} denotes the cooling or heating output of the AC system, Q_{occ} denotes the heat released from people, Q_{eq} denotes the heat released from equipment, $Q_{envelop}$ denotes the heat transferred from the outdoors to the indoors through the building envelope, Q_{air} denotes the heat gain and loss of

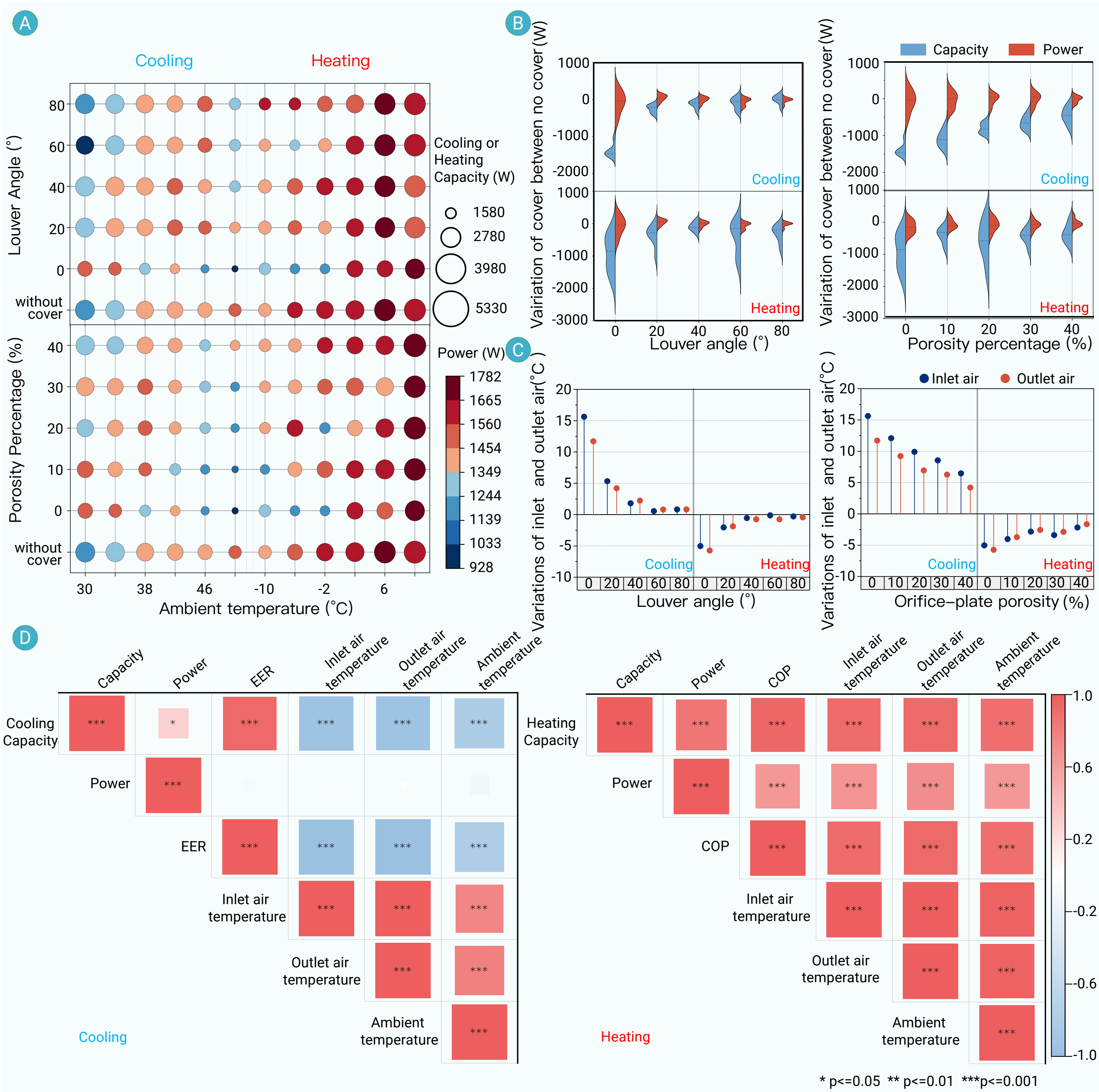

Figure 3. Impact of covers on energy performance (A) Cooling and heating performance under varying louver angles (0°–80°) and orifice-plate porosities (0%–40%). (B) Cooling and heating capacity and power changes with louver angles and porosities, compared to uncovered units. (C) Effect of louver angle and porosity percentage on the temperature difference at the inlet of the outdoor unit, comparing covered and uncovered conditions. (D) Relationships among outdoor unit inlet/outlet temperatures, ambient temperature, and energy performance.

air within the building. Given the significant impact of building functions on Q_{occ} and Q_{eq}, and the focus on heat transfer within and between buildings in diverse climate contexts, it is prudent to exclude these variables from consideration. Consequently, we can express the relationship as follows:

$$Q_{AC} = Q_{envelop} + Q_{air} \quad (2)$$

The equation is expressed as follows:

$$c\times m\times\left(T^{0}_{room}-T_{room}\right) = \int \alpha\times\tau\times d\tau - \int\left(\frac{A_{wall}}{R_{wall}}+\frac{A_{window}}{R_{window}}\right)\left(T_{outdoor}-T_{room}\right)\times d\tau \quad (3)$$

In the equation, c represents the specific heat capacity of the indoor air, m denotes the mass of the indoor air, T^{0}_{room} is the initial indoor air temperature, T_{room} is the indoor air temperature at a given moment, τ is the slope of the cooling capacity versus time curve obtained experimentally, τ is the time, A_{wall} and A_{window} are the areas of the wall and window, respectively, R_{wall} and R_{window} are the thermal resistances of the wall and window, respectively, and $T_{outdoor}$ is the outdoor ambient temperature. Therefore, solving the above equation

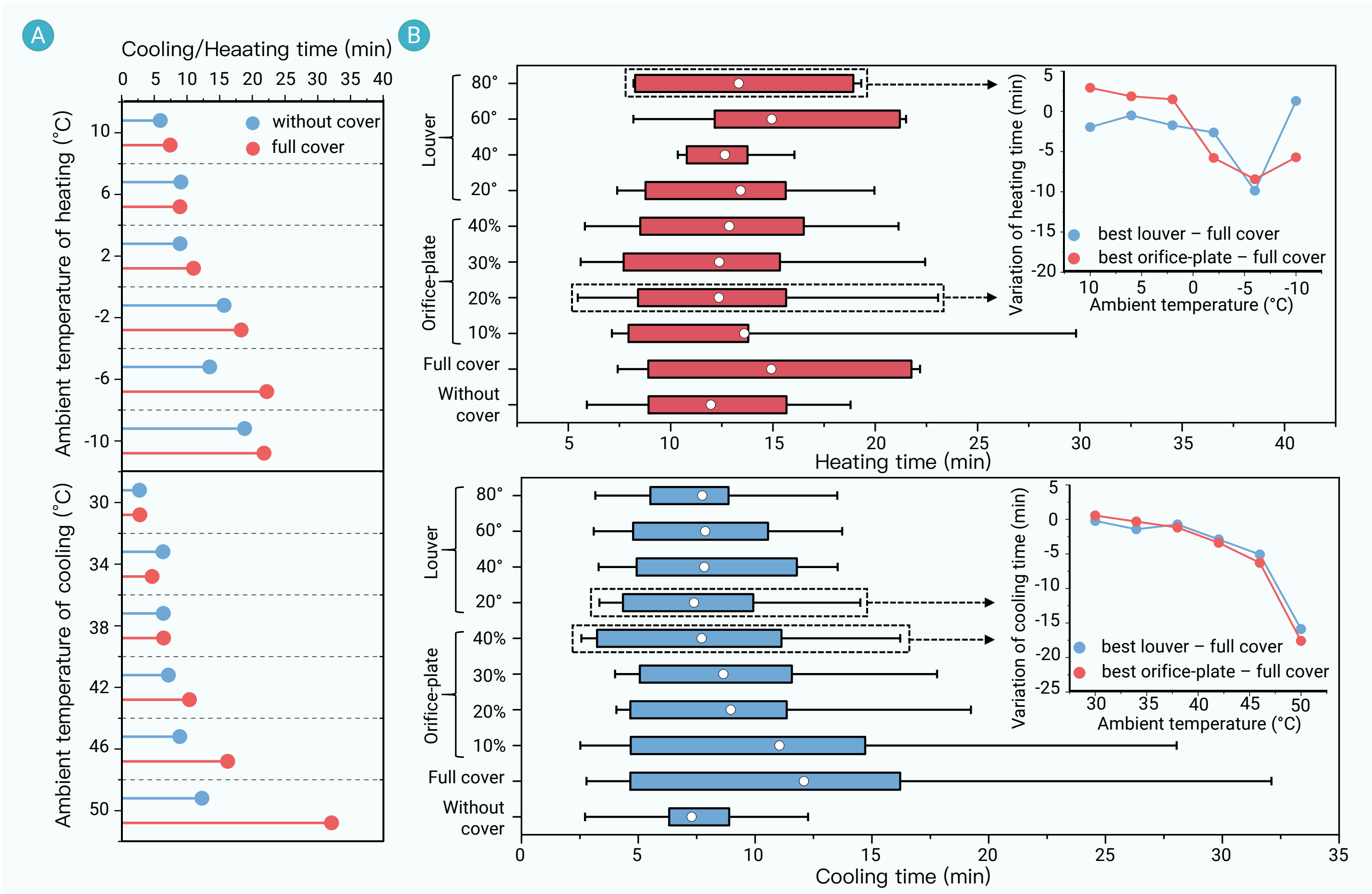

Figure 4. Cover effect on AC cooling and heating times (A) Cooling and heating time of the fully covered and uncovered units, across a range of ambient temperatures from 30°C to 50°C and from 10°C to -10°C. (B) Distribution of cooling and heating times under varying louver angles and porosity percentages across the test's ambient temperatures and structural parameters with minimal adverse effects.

yields:

$$-c\times m\times\frac{d\left(T_{room}\right)}{d\tau}=\alpha\times\tau-\left(\frac{A_{wall}}{R_{wall}}+\frac{A_{window}}{R_{window}}\right)\left(T_{outdoor}-T_{room}\right)\quad(4)$$

The equation is a first-order linear homogeneous differential equation T_{room} as the dependent variable and τ as the independent variable. This equation can be solved using Matlab software. Similarly, in the winter season, for the first scenario, we have:

$$c\times m\times\frac{d\left(T_{room}\right)}{d\tau}=\alpha\times\tau-\left(\frac{A_{wall}}{R_{wall}}+\frac{A_{window}}{R_{window}}\right)\left(T_{room}-T_{outdoor}\right)\quad(5)$$

In the summer season, for the second scenario:

$$c\times m\times\left(T^{0}_{room}-T_{room}\right)=P^{0}_{cool}\times\tau^{1}\times\frac{1}{2}+\int P^{0}\times d\left(\tau-\tau^{1}\right)-\int\left(\frac{A_{wall}}{R_{wall}}+\frac{A_{window}}{R_{window}}\right)\left(T_{outdoor}-T_{room}\right)\times d\tau\quad(6)$$

In the equation, P^{0}_{cool} represents the stable cooling capacity of the AC system as measured in the laboratory, and τ^{1} denotes the time required for the AC system to reach stability from the moment it is activated, also determined experimentally. Similarly, in the winter season, for the second scenario, we have:

$$c\times m\times\left(T_{room}-T^{0}_{room}\right)=P^{0}_{cool}\times\tau^{1}\times\frac{1}{2}+\int P^{0}\times d\left(\tau-\tau^{1}\right)-\int\left(\frac{A_{wall}}{R_{wall}}+\frac{A_{window}}{R_{window}}\right)\left(T_{room}-T_{outdoor}\right)\times d\tau\quad(7)$$

By employing the equations, solutions are obtained using Matlab software.

Building Energy Simulation and Analysis. This study utilizes whole-building energy simulation and geographic analysis to evaluate the regional energy and operational impacts of AC covers across Asia. Using EnergyPlus and batch processing via Python, the analysis assesses outcomes including annual cooling energy consumption and cumulative cooling operation time. Results are spatially aggregated to quantify cover-induced penalties across climate zones and identify optimal design parameters.

Energy simulations were performed using the ASHRAE 90.1 high-rise apartment model as the base IDF file, adjusted within EnergyPlus to reflect the desired building parameters. Weather data encompassing all available locations in Asia (WMO Region 2) were obtained from the EnergyPlus Weather Database (https://energyplus.net/weather) and incorporated into the simulations. Automated batch processing was implemented via the eppy Python library to systematically execute simulations across all climatic conditions. The building model, adapted from the ASHRAE reference, as shown in Figure S2, represents a high-rise residential structure with key characteristics including a south-oriented façade, 10 stories, a total floor area of 7,840 m^2, and a window-to-wall ratio of 30%. The HVAC system was configured as a packaged terminal heat pump (PTHP), with cooling and heating setpoints maintained at 28°C and 20°C, respectively.

RESULTS

Impact of cover structures on AC energy performance

As illustrated in Figure 3A there was a notable decline in both EER and cooling capacity as the ambient temperature increased from 30°C to 50°C, even without a cover. The EER exhibited a decline of 46%, from 3.84 to 2.08, while the cooling capacity demonstrated a reduction of 34%, from 4,657 W to 3,056 W. In contrast, the power rose by 21%, from 1,212 W to 1,472 W, highlighting the reduced energy performance at higher ambient temperatures.

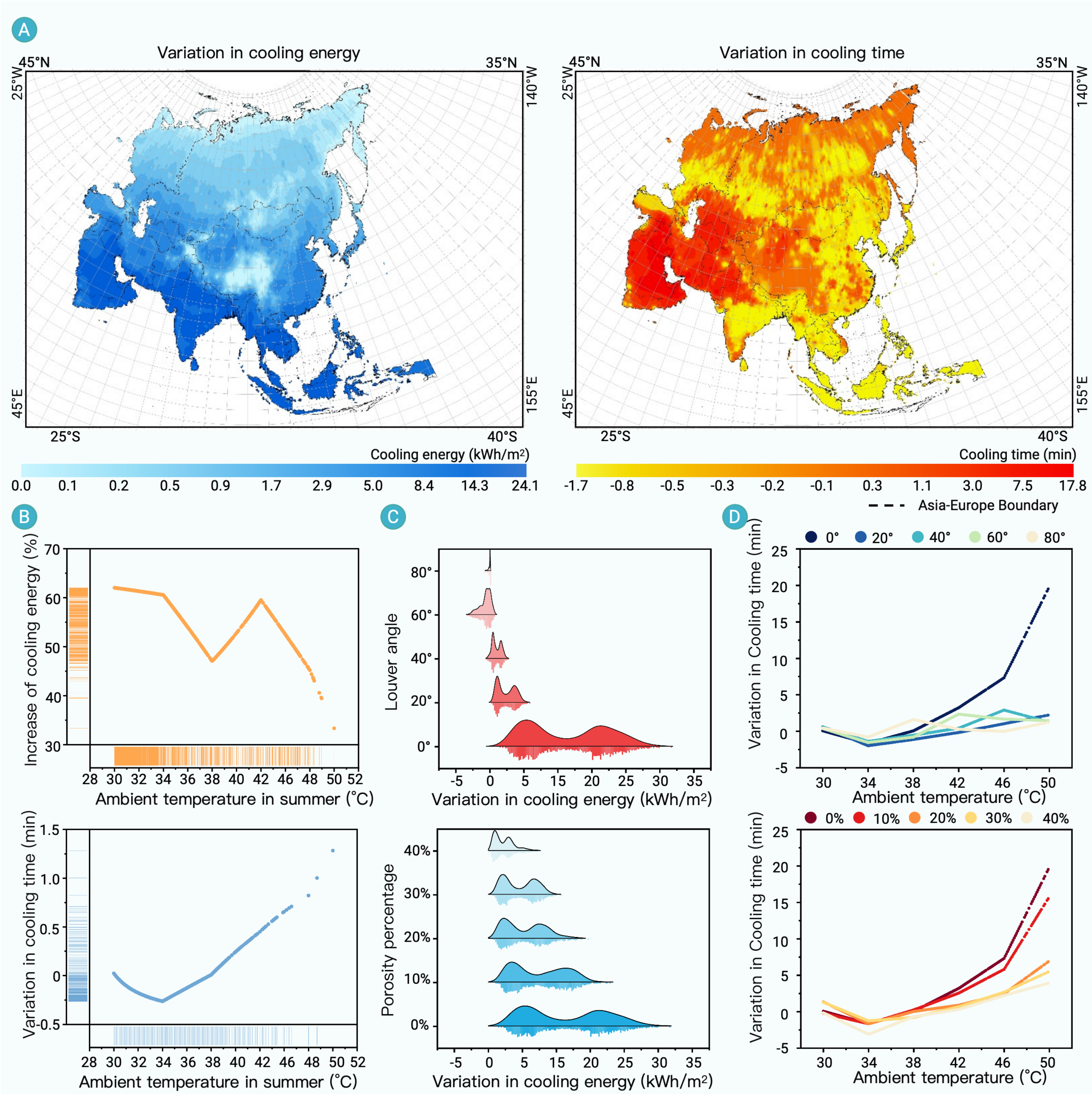

Figure 5. Impact on building in Asia (A) Distribution of the impact of fully covered air conditioner units on cooling energy compared to uncovered units across Asia. (B) Distribution of the impact of fully covered air conditioner units on cooling time compared to uncovered units across Asia. (C) Increase in cooling energy and time of fully covered units compared to uncovered units at different ambient temperatures. (D) Vairations in cooling energy compared to uncovered conditions under different louvre angles and porosity percentages. (E) Vairations in cooling time compared to uncovered conditions under different louvre angles and porosity percentages.

Similarly, as the ambient temperature decreased from 10°C to -10°C in heating seasons, the COP declined by 33%, from 3.31 to 2.22, and the heating capacity decreased by 40%, from 5,216 W to 3,150 W. At a temperature below 2°C, the air outlet temperature fell below 0°C, thereby initiating the defrost operation mode. Additionally, the power demand decreased in response to low ambient temperature, declining by 8% from 1,574 W to 1,421 W as the system engaged low-pressure protection to safeguard the compressor. At higher temperatures, high-pressure protection limited the power output, a phenomenon that was also observed with covers. Figure 3B lustrates that covers reduce both cooling and heating capacities, as well as power demand, in comparison to units without covers. Louver covers resulted in a reduction of 377 W and 917 W in cooling and heating capacities, while cooling and heating power declined by 21 W and 69.3 W, on average. This resulted in a decrease of 0.26 in EER and 0.16 in COP. The orifice-plate covers caused a reduction in cooling and heating capacities of 876 W and 534 W, respectively, accompanied by a decrease in cooling and heating power of 30 W and 77 W, on average. This led to declines in EER and COP by 0.64 and 0.24, respectively. However, as the louver angle and the orifice-plate porosity increased, the negative impact on AC energy performance lessened. To illustrate, at a louver angle of 80°, cooling and heating capacities increased by 1,384 W and

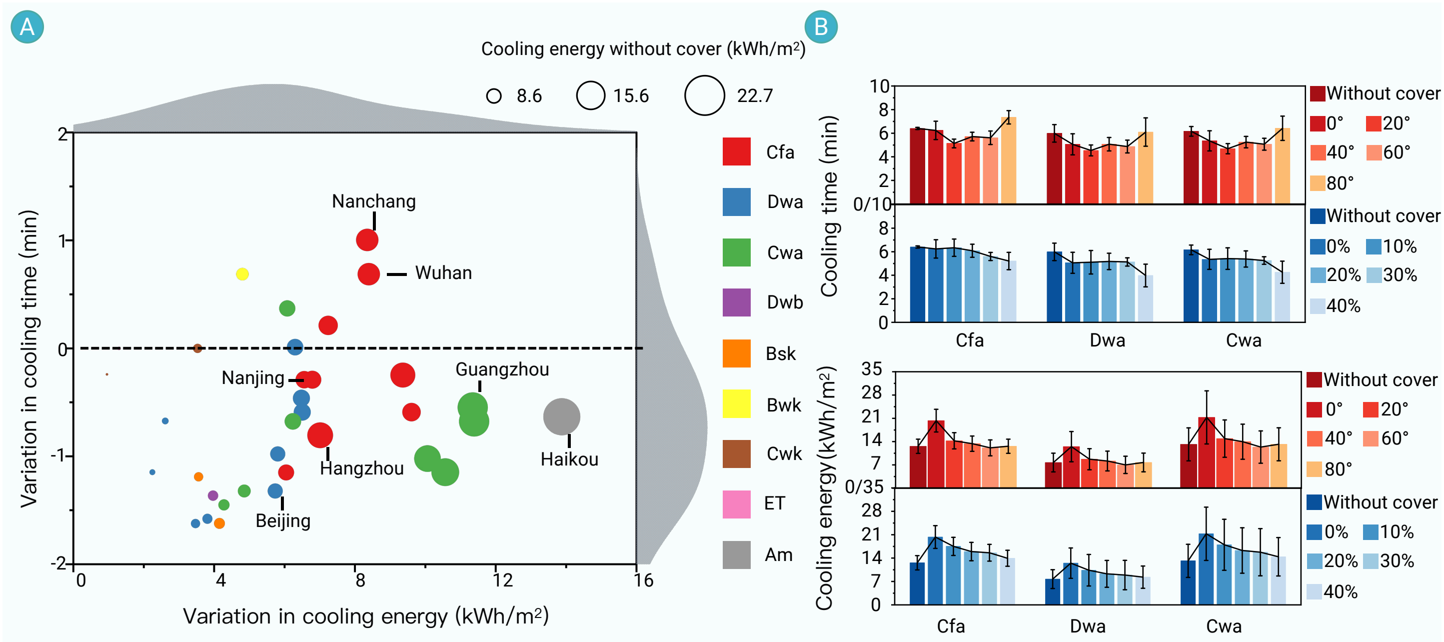

Figure 6. Impact on building in different climate zones of China (A) Variations in cooling energy and cooling time induced by fully covered compared to uncovered outdoor units in China under Köppen climate classification. (B) Distribution of cooling time and energy under different structural parameters of louver and orifice-plate covers in three major climate zones of China (Cfa, Dwa and Cwa).

614 W, respectively, in comparison to a fully covered case. Similarly, an orifice-plate porosity of 40% allowed for an increase in cooling and heating capacities of 936 W and 563 W, respectively.

To understand the operational impacts of covers on AC systems, a correlation analysis was conducted using experimental data. The primary effect of cover installation is the restriction of airflow from the outdoor unit's air outlet. This restricted air is then recirculated via the inlet, where it exchanges heat with the condenser. In summer, the air is warmer than the surrounding environment, whereas in winter, it is cooler. As a result, the cover creates a localized temperature difference, causing the air temperature around the unit to exceed ambient levels in summer and drop below them in winter. This impact varies inversely with the structural parameters of covers. Reducing the louver angle and orifice-plate porosity minimizes the difference between the inlet and outlet temperature compared to the uncovered cases at the same ambient temperature,as shown in Figure 3C

As illustrated in Figure 3D, in summer, the AC cooling capacity exhibited a negative correlation with both EER and the inlet and outlet air temperatures, with a Pearson's coefficient of less than -0.95. In contrast, in winter, the heating capacity and COP demonstrated a positive correlation with those temperatures. The compressor, as the primary power source, exhibited a distinct operational profile under the influence of seasonal protections. In summer, when high-pressure protection is triggered, the power is inversely correlated with the inlet and outlet temperatures. Without protection, this correlation becomes positive. Conversely, in winter, low-pressure protection correlates power positively with inlet and outlet temperatures, while units without protection reverses this relationship. The experimental data further reveal that heating conditions within the tested temperature range activate compressor protection more frequently than cooling conditions. Therefore, there was no significant correlation between the power and the inlet and outlet temperatures in summer; however, a strong positive correlation was observed in winter.

Impact of cover structures on AC cooling and heating time

As the ambient temperature rose from 30°C to 50°C, the AC system could cool the indoor air temperature to the target temperature of 28°C. However, it should be noted that the cooling time increases linearly with the widening temperature difference between the indoor and outdoor air. Figure 4A shows that without a cover, cooling time extended significantly, from 2.72 minutes at 30°C to 12.70 minutes at 50°C. The installation of a cover resulted in an additional increase in cooling time, as illustrated in Figure 4A. When fully covered, cooling from 30°C to the target temperature took 2.78 minutes, while from 50°C, it extended to 32.10 minutes (an increase of more than 160% from the 30°C case). This will have an adverse effect on user comfort. Although adding a cover increases cooling time at all ambient temperatures, changes to the cover's structural parameters can mitigate this effect. An increase in louver angle from 0° to 80° reduced the average cooling time by 36%, from 12.09 to 7.74 minutes. Similarly, an increase in orifice-plate porosity from 0% to 40% reduced the average cooling time from 12.09 to 7.72 minutes. Therefore, as the ambient temperature rises, a larger louver angle and higher orifice-plate porosity become more optimal.

As illustrated in Figure 4A, when the ambient temperature declined from 10°C to -10°C, the AC system could elevate the indoor temperature to the target temperature of 20°C. However, the heating time increases as the ambient temperature declines, regardless of whether a cover is installed. Without a cover, the heating time increased from 5.91 minutes at 10°C to 18.80 minutes at -10°C. When fully covered, the heating time was further extended, from 7.41 minutes at 10°C to 21.77 minutes at -10°C, with an average increase of 2.96 minutes compared to the uncovered condition. It is evident that the impact on heating time is significant but differs from the effect in the cooling condition. As illustrated in Figure 4B, the mean heating time declines initially and then increases as the louver angle and orifice-plate porosity are augmented. Among the tested variables, a 40° louver angle yielded the shortest average heating time, at 12.65 minutes, while a porosity of 20% resulted in the shortest heating time, at 12.36 minutes. This represented an increase of only 0.68 minutes and 0.39 minutes, respectively, compared to the uncovered condition, as shown in Figure 4B.

In this test, the ideal temperature settings were used for indoor cooling (28°C) and heating (20°C), respectively. The AC operational time will increase with covers on the outdoor units and to meet a lower temperature for cooling (e.g., 22°C–28°C) or a higher temperature for heating (e.g., 20°C–26°C).

Impact of cover structures on cooling energy and time in Asia under different climate zones

Study findings reveal that across Asia, fully enclosed covers increase cooling energy consumption and cooling time by an average of 11.4 kWh/m^2 and 0.1 min, respectively, compared to uncovered scenarios, with maximum observed increases of 26.6 kWh/m^2 and 19.5 min. The spatial distribution of impacts from full enclosure is detailed in Figure 5A and Figure 5B. Notably,

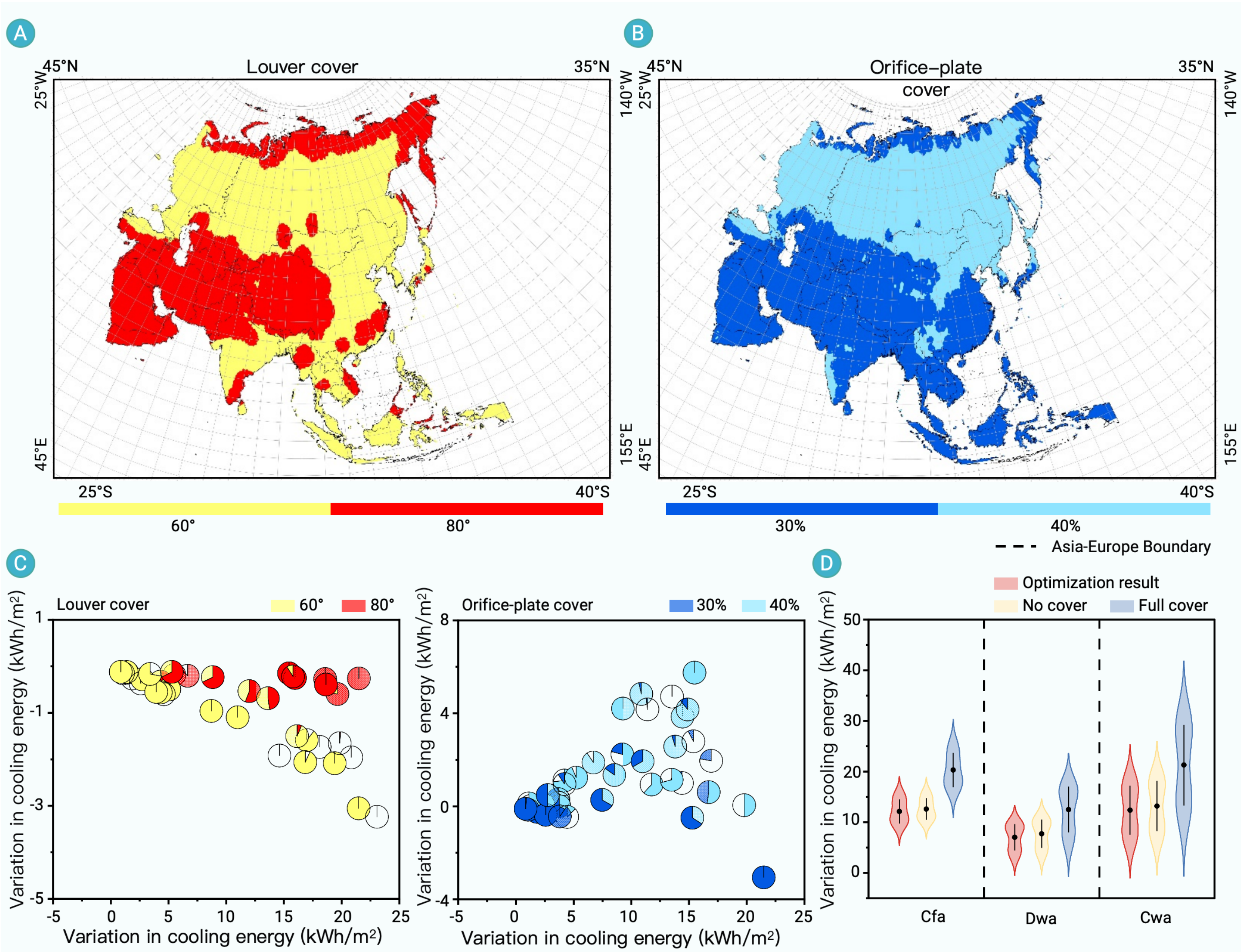

Figure 7. Optimal design of cover in Asia (A) Optimal louver angle for countries in Asia. (B) Optimal orifice-plate porosity for countries in Asia. (C) Comparison analysis of cooling energy under the optimized louver and orifice-plate covered conditions with fully covered (x-axis) and uncovered (y-axis) conditions in Asian countries. (D) Comparison analysis of cooling energy under the optimized louver covered conditions with fully covered in three main three major climate zones of China under Köppen climate classification (Cfa, Dwa and Cwa).

nations with higher average summer temperatures - such as India, Iran, and Saudi Arabia - experience disproportionately severe energy penalties, with average increases of 15.3, 8.6, and 15.6 kWh/m^2, respectively. In these regions, elevated ambient temperatures force AC systems to operate for extended durations under thermally stressful conditions to meet residential cooling demand; cover installation unequivocally exacerbates this operational strain.Figure 5C illustrates the percentage increase in cooling energy consumption attributable to full enclosure across varying summer average temperatures. Within the predominant temperature range of 30-36°C - where most Asian populations reside-covers elevate cooling energy use by approximately 60%, representing substantial avoidable waste. Figure 5C further demonstrates that above an extreme temperature threshold of 34°C, the incremental increase in cooling time intensifies with rising ambient heat. Iran, Saudi Arabia, and Afghanistan exhibit particularly pronounced impacts, with cooling time extensions averaging 2.6, 6.1, and 2.2 min during extreme heat events.

Crucially, cover structural parameters profoundly influence both building energy demand and extreme-heat cooling performance. As shown in Figure 5D, increasing the louver angle from 0° to 80° reduces the average cooling energy penalty (relative to uncovered units) from +11.4 to +0.0 kWh/m^2 - a net improvement of 11.4 kWh/m^2. Similarly, raising orifice-plate porosity from 0% to 40% decreases this penalty from +11.4 to +2.3 kWh/m^2 (9.1 kWh/m^2 improvement). These optimizations concurrently mitigate extreme-heat cooling time delays, as shown in Figure 5E. While cooling time inherently rises with temperatures exceeding 34°C regardless of configuration, increased louver angles and porosities significantly curb this escalation. Specifically, increasing the louver angle from 0° to 80° reduces the maximum cooling time increment (vs. uncovered) from 19.5 to 1.6 min (17.9 min improvement). For orifice-plate cover, raising porosity from 0% to 40% decreases this increment from 19.5 to 3.9 min (15.6 min improvement). The superior adjustability of louver cover (achieving near 90° angles) enables performance closer to the uncovered baseline, yielding more pronounced energy benefits than orifice-plate cover.

Focusing on China - Asia's most severely affected nation - we analyzed cover impacts across Köppen climate zones in 34 provincial capitals, as shown in Figure 6A. Within China's three dominant climate types (Cfa, Dwa, Cwa), the Cwa zone (encompassing Guangzhou) experienced the highest average energy penalty (+8.1 kWh/m^2). While cooling time decreased overall under full enclosure in China's relatively moderate summer extremes, it increased by 1.0 min and 0.7 min in hotter Cwa cities like Nanchang and Wuhan, respectively. Critically, despite reduced cooling time penalties continent-wide, the absolute energy waste in China remains severe and scales proportionally with baseline uncovered consumption. Parameter optimization analysis, as shown in Figure 6B. demonstrates that a 60° louver angle minimizes impacts across all three major climate zones, reducing the energy penalty by 7.5 kWh/m^2 relative to full enclosure. A 40% orifice-plate porosity similarly reduces penalties by 5.8 kWh/m^2. Increasing louver angles and porosities consistently diminishes negative impacts across zones. Figure 6B confirms that a 20° louver angle and 40% porosity maximize cooling time reductions versus full enclosure (1.1 min and 1.3 min improvement, respectively).

Cover design recommendations for different climate regions

Building upon the aforementioned analysis, this study proposes design recommendations for AC covers. Aiming to minimize the impact of covers on summer cooling energy demand, this study statistically determined the optimal cover design parameters for locations throughout Asia. We present the spatial distribution of optimal parameters for louver and orifice-plate covers across Asian regions in Figure 7A and Figure 7B, respectively. The optimal louver angles are 60° and 80°, while optimal orifice-plate porosities are 30% and 40%. Geographically, the 80° louver angle is predominantly distributed across central and western Asia (e.g., Afghanistan, Iran, Saudi Arabia), whereas the 60° angle prevails in eastern and northern Asia (e.g., Russia, China, Japan, Indonesia). For orifice-plate covers, a porosity of 30% is primarily found south of Russia and Mongolia, while Russia and Mongolia exhibit a predominant optimal porosity of 40%.

We quantified the contribution of optimal parameter designs in mitigating the negative impacts of covers on cooling energy consumption, as illustrated in Figure 7C. Statistical analysis across Asian nations reveals that optimal louver and orifice-plate designs reduce cooling energy use by an average of 11.1 kWh/m^2 and 8.9 kWh/m^2, respectively, compared to fully enclosed covers. Crucially, relative to uncovered scenarios, optimal louvers result in a marginal average reduction of 0.8 kWh/m^2, while optimal orifice plates incur a slight average increase of 1.3 kWh/m^2. For louver covers, the optimized design yields cooling energy consumption lower than the uncovered baseline in specific regions. For instance, in China, optimal louver parameters reduce consumption by 0.5 kWh/m^2 relative to uncovered units and by 5.1 kWh/m^2 relative to full enclosure. This counterintuitive benefit stems from optimized covers enhancing AC system operational efficiency under specific conditions, thereby lowering summer energy demand. Orifice-plate covers with optimal porosity exhibit a small energy increase (e.g., +0.3 kWh/m^2 in China) relative to uncovered units but achieve a substantial reduction (-4.2 kWh/m^2) compared to full enclosure, effectively minimizing their negative impact.

Analysis further indicates regional heterogeneity within nations. For example, in India, optimal parameters vary: 10.7% of regions recommend a 60° louver angle, while the remainder recommend 80°. Comparative assessment demonstrates that a 60° louver angle and 30% orifice-plate porosity generally yield smaller negative impacts or even positive net effects on cooling energy consumption. Focusing on China's major Köppen climate classifications (Cfa, Dwa, Cwa), Figure 7D shows that optimal louver designs achieve near parity with uncovered scenarios, with differences of only -0.5, -0.7, and -0.8 kWh/m^2, respectively. While optimal orifice-plate designs exhibit less favorable energy performance than optimal louvers, they nonetheless demonstrate significant optimization benefits, reducing consumption by 6.3, 4.4, and 7.1 kWh/m^2 compared to full enclosure.

DISCUSSION

The energy penalties imposed by AC unit covers exhibit marked heterogeneity across Asian countires, with implications for both energy security and equitable urban development.[33] Taking China as an example, the energy and economic penalties are substantial. In Beijing (Dwa climate zone), fully enclosed covers increased annual cooling energy demand by 5.7 kWh/m^2, translating to a 3.4 RMB/m^2 seasonal cost escalation (at 0.6 RMB/kWh[34]). The penalty soared to 11.35 kWh/m^2 (6.81 RMB/m^2) in Guangzhou's subtropical climate, where cooling dominates year-round. For mixed climates like Shanghai, combined cooling and heating inefficiencies raised annual cooling costs by 3.63 RMB/m^2. Scaling this up nationally, fully enclosed covers cause an average increase of 4.26 kWh/m^2 across China. Given the vast Chinese residential floor area of 1.07 × 10^{11} m^2, this translates to an alarming national energy waste of 4.56 × 10^{11} kWh annually, corresponding to an estimated 260 million tons of additional CO_2 emissions.[35] This quantification underscores not only the regressive economic burden on households but also the profound environmental impact at a national scale. Moreover, fully enclosed covers significantly prolong the cooling time required for air conditioning systems in nations experiencing frequent extreme heat events. For instance, in Saudi Arabia—a nation where peak summer temperatures average 43.9°C—cooling time increases significantly from 8.0 min (uncovered) to 14.1 min (fully covered), representing a 76.3% increase. Moreover, user behaviors—such as setting lower temperatures to compensate for delayed cooling—may amplify energy demand, mirroring feedback mechanisms. Additionally, covers contribute to increased noise levels from external units,[37] further highlighting their negative environmental impacts.

Considering the greater negative impacts of covers on AC systems in regions where AC is in much more demand, both for cooling in summer and heating in winter, it is not recommended to cover the outdoor units, except for special reasons such as the aesthetic view requirements of historical buildings. If AC covers are required, our study demonstrates that optimized cover designs can mitigate these trade-offs. Our results demonstrate that louvered covers (60°/80° angles) and orifice plates (30%/40% porosity) limit cooling energy penalties to less than 1.5 kWh/m^2 while preserving visual coherence. This performance stems from these specific parameters creating sufficient open area to minimize airflow resistance and hot-air entrapment. By codifying these clear, prescriptive parameters, policymakers can effectively eliminate the energy penalty of aesthetic covers without the need for complex case-by-case assessments. Notably, in China, the implementation of optimized louver designs (with a 60° angle) reduces average annual cooling energy consumption by 0.5 kWh/m^2 compared to scenarios without any cover. The optimized louver designs can reduce 4.021011 kWh of energy consumption and 229,260 million tons of CO_2 emissions compared to the situation of complete covering. Therefore, optimized structural parameters can achieve a significant reduction in cooling energy consumption and carbon emissions.

The use of covers worsens AC system operating conditions and leads to increased power consumption and extended run times, which, in turn, elevate the power grid's peak load during high-demand periods. This situation hinders the sustainable development of the building sector and may obstruct China's progress toward its sustainability goals.[38] Additionally, when facing an extremely hot or cold climate,[39] older AC units may experience breakdowns because they must run longer at peak power, which can also result in underheating or undercooling, thus increasing occupants' thermal discomfort. Furthermore, the increased energy consumption and associated costs caused by the use of covers could lead to issues of fairness within communities, as some residents experience higher electricity bills.[40,41] Urban planners and city policy makers should be aware of the impacts of covers on energy use and environmental impacts when making policy or establishing regulations on AC covers. Therefore, a strategic approach integrating optimized cover designs (60°/80° louver angles or 30%/40% porosities) with appropriate unit placement (0.15 m front and 0.2 m side) is essential to reconcile energy performance with urban aesthetics. Building codes and energy standards should mandate these specific parameters to provide clear, evidence-based guidelines, ensuring that covers achieve both functional efficiency and visual coherence when their use is unavoidable.

However, several limitations must be acknowledged. First, while our experiments spanned Asian major climate zones, microclimatic variations in high-rise urban environments may alter cover performance—a critical consideration given the rise of vertical urbanization. Second, the long-term impacts of cyclic thermal stress on compressor lifespan remain unquantified; accelerated degradation could offset short-term efficiency gains. Third, our humidity controls adhered to national standards, yet monsoon-driven moisture extremes in southern Asia may exacerbate latent load penalties under covers[42-44]. To address the multiscale challenges of energy waste, extreme heat performance loss, and grid stress identified in this study, future research should prioritize adaptive cover solutions. For instance, dynamic louvers could adjust their angle based on ambient temperature and AC operation, optimizing both airflow and aesthetics. Integrating phase-change materials into cover designs could passively absorb and dissipate excess heat, mitigating the local microclimate temperature rise around the outdoor unit. The deployment of such solutions are critical for mitigating Asia's severe and growing cooling deficit, as exemplified by India. With continued population growth and climate change, demand for air conditioning will escalate substantially—for instance, China projects a 41% increase by 2050[23]. This study provides a critical pathway to reconcile future AC deployment with urban planning imperatives, advancing sustainable strategies for low-carbon cities.

CONCLUSION

This study provides a comprehensive quantification of the substantial energy burden imposed by aesthetic façade covers on outdoor air conditioner units across Asia. Our integrated methodology, combining laboratory experiments, thermodynamic modeling, and continental-scale energy simulations, unequivocally demonstrates that fully enclosed covers severely degrade AC performance. They increase building cooling energy consumption by an average of 11.4 kWh/m^2 and critically extend cooling operation times, exacerbating peak electricity demand during extreme heat events.

The core finding of this work is that these significant energy penalties are entirely avoidable through optimized cover designs. We have identified and validated specific structural parameters that can virtually eliminate the efficiency loss: louver covers with angles of 60° or 80°, and orifice-plate covers with porosities of 30% or 40%. These optimized designs reduce the cooling energy penalty to a marginal level, achieving a near-net-zero impact compared to uncovered units—while maintaining the visual coherence of building facades.

Therefore, we issue the following clear recommendations:

1. The most energy-efficient policy is to avoid installing covers on outdoor AC units.

2. Where covers are deemed necessary for urban aesthetics, building codes, facade standards, and municipal regulations must mandate the use of these optimized parameters (60°/80° louver angles or 30%/40% orifice-plate porosities).

Looking forward, the integration of these evidence-based designs into urban policy presents an immediate and viable pathway for Asian megacities to reconcile urban aesthetics with urban energy consumption.

REFERENCES

1. Chen K., Lin H., Shyr O. F., et al. (2023). What are the differences in urban citizens' preferences for the colour of condominium building facades. *Human. Social Sci. Commun.* 10:833. DOI:10.1057/s41599-023-02372-9
2. Kong G. and Fan H. (2020). Enhanced Facade Parsing for Street-Level Images Using Convolutional Neural Networks. *IEEE TGRS* PP:1-13. DOI:10.1109/TGRS.2020.3035878
3. Xiang C. and Matusiak B. S. (2022). Façade Integrated Photovoltaics design for high-rise buildings with balconies, balancing daylight, aesthetic and energy productivity performance. *J. Build. Eng.* 57:104950. DOI:10.1016/j.jobe.2022.104950
4. Xue X., Tian Z., Yang Y., et al. (2025). Sustaining the local color of a global city. *Nat. Cities* 2:400–412. DOI:10.1038/s44284-025-00225-x
5. Zhang Z., Hui H. and Song Y. (2025). Mitigating the vicious cycle between urban heatwaves and building energy systems in Guangdong–Hong Kong–Macao Greater Bay Area. *Innov. Energy* 2:100080. DOI:10.59717/j.xinn-energy.2025.100080
6. Ornam K., Wonorahardjo S. and Triyadi S. (2024). Several façade types for mitigating urban heat island intensity. *Build. Environ.* 248:111031. DOI:10.1016/j.buildenv.2023.111031
7. Pineda-Zumaran J. and Alpaca-Chavez M. (2024). Revisiting façade design and its contribution to the urban experience in the 21st century. *J. Urban Design* 29:735–752. DOI:10.1080/13574809.2024.2348553
8. Yi Y. K. (2019). Building facade multi-objective optimization for daylight and aesthetical perception. *Build. Environ.* 156:178–190. DOI:10.1016/j.buildenv.2019.04.002
9. Davis L., Gertler P., Jarvis S., et al. (2021). Air conditioning and global inequality. *Global Environ. Change* 69:102299. DOI:10.1016/j.gloenvcha.2021.102299
10. Pavanello F., De Cian E., Davide M., et al. (2021). Air-conditioning and the adaptation cooling deficit in emerging economies. *Nat. Commun.* 12:6460. DOI:10.1038/s41467-021-26592-2
11. Wang W., Deng Y., Wu J., et al. (2024). The hidden costs of concealing outdoor air conditioning units. *Nat. Cities* 1:722–724. DOI:10.1038/s44284-024-00148-z
12. Davis L. W. and Gertler P. J. (2015). Contribution of air conditioning adoption to future energy use under global warming. *PNAS* 112:5962–5967. DOI:10.1073/pnas.1423558112
13. Isaac M. and van Vuuren D. P. (2009). Modeling global residential sector energy demand for heating and air conditioning in the context of climate change. *Energy Policy* 37:507–521. DOI:10.1016/j.enpol.2008.09.051
14. Levesque A., Pietzcker R. C., Baumstark L., et al. (2018). How much energy will buildings consume in 2100. *A global perspective within a scenario framework. Energy* 148:514–527. DOI:10.1016/j.energy.2018.01.139
15. Biardeau L. T., Davis L. W., Gertler P., et al. (2020). Heat exposure and global air conditioning. *Nat. Sustain.* 3:25–28. DOI:10.1038/s41893-019-0441-9
16. IEA. (2018). The Future of Cooling. Prepirnt at https://www.iea.org/reports/the-future-of-cooling
17. IEA. (2021). Air conditioning units in operation by region, 2000-2020. Preprint at https://www.iea.org/data-and-statistics/charts/air-conditioning-units-in-operation-by-region-2000-2020
18. Afram A. and Janabi-Sharifi F. (2014). Review of modeling methods for HVAC systems. *Appl. Therm. Eng.* 67:507–519. DOI:10.1016/j.applthermaleng.2014.03.055
19. Sadeghianjahromi A. and Wang C.-C. (2021). Heat transfer enhancement in fin-and-tube heat exchangers – A review on different mechanisms. *Renew. Sustain. Energy Rev.* 137:110470. DOI:10.1016/j.rser.2020.110470
20. Yuan Y., Zhang N., Tao W., et al. (2014). Fatty acids as phase change materials: A review. *Renew. Sustain. Energy Rev.* 29:482–498. DOI:10.1016/j.rser.2013.08.107
21. Staffell I., Pfenninger S. and Johnson N. (2023). A global model of hourly space heating and cooling demand at multiple spatial scales. *Nat. Energy* 8:1328–1344. DOI:10.1038/s41560-023-01341-5
22. Deroubaix A., Labuhn I., Camredon M., et al. (2021). Large uncertainties in trends of energy demand for heating and cooling under climate change. *Nat. Commun.* 12:5197. DOI:10.1038/s41467-021-25504-8
23. Falchetta G., Cian E. D., Pavanello F., et al. (2024). Inequalities in global residential cooling energy use to 2050. *Nat. Commun.* 15:7874. DOI:10.1038/s41467-024-52028-8
24. Pandey B., Brelsford C. and Seto K. C. (2025). Rising infrastructure inequalities accompany urbanization and economic development. *Nat. Commun.* 16:1193. DOI:10.1038/s41467-025-56539-w
25. Wu J., Wang L., Hong T., et al. (2024). Revealing and optimizing the design of cover installation for outdoor units of air conditioners through CFD simulations and thermodynamic modeling. *J. Build. Eng.* 87:109014. DOI:10.1016/j.jobe.2024.109014
26. Nada S. A. and Said M. A. (2017). Performance and energy consumptions of split type air conditioning units for different arrangements of outdoor units in confined building shafts. *Appl. Therm. Eng.* 123:874–890. DOI:10.1016/j.applthermaleng.2017.05.104
27. Chow T. T., Lin Z. and Yang X. Y. (2002). Placement of condensing units of split-type air-conditioners at low-rise residences. *Appl. Therm. Eng.* 22:1431–1444. DOI:10.1016/S1359-4311(02)00068-6
28. Xue H., Xu B., Wu J., et al. (2007). Prediction of temperature rise near condensing units in the confined space of a high-rise building. *Build. Environ.* 42:2480–2487. DOI:10.1016/j.buildenv.2006.06.011
29. Kwag B. C., Kim G. T. and Im D. (2023). Evaluation of the impact of installation environment for a condensing unit of a split-type air conditioner in a plant room of Korean apartment dwellings. *Int. J. Refrig.* 156:207–218. DOI:10.1016/j.ijrefrig.2023.10.002
30. Bruelisauer M., Meggers F., Saber E., et al. (2014). Stuck in a stack—Temperature measurements of the microclimate around split type condensing units in a high rise building in Singapore. *Energy Build.* 71:28–37. DOI:10.1016/j.enbuild.2013.11.056
31. Meyer D., Schoetter R. and van Reeuwijk M. (2024). Energy and environmental impacts of air-to-air heat pumps in a mid-latitude city. *Nat. Commun.* 15:5474. DOI:10.1038/s41467-024-49836-3
32. He P., Liu P., Qiu Y., et al. (2022). The weather affects air conditioner purchases to fill the energy efficiency gap. *Nat. Commun.* 13:5772. DOI:10.1038/s41467-022-33531-2
33. Mubiinzi G., Senyonga L., Kaawaase T. K., et al. (2024). Income and price elasticities of household electricity demand: A comparative systematic review of aggregated and disaggregated data studies. *Energy Rep.* 12:4449–4465. DOI:10.1016/j.egyr.2024.10.021
34. Wang S. R., Mo J. L., Yang J., et al. (2025). Scenario-based projections of electricity prices in China's carbon-neutral transition. *iscience* 28. 112958,DOI:10.1016/j.isci.2025.112958
35. Liu X. M., Zhu T. S., Cai W. G., et al. (2025). Carbon emission efficiency of urban residential buildings in China: a study based on a three-stage DEA model. *Eng. Const. Arch. Manag.*:1–23. DOI:10.1108/ECAM-09-2024-1234
36. Li R., Hu Y., Wang X., et al. (2024). Estimating the impacts of a new power system on electricity prices under dual carbon targets. *J. Clean. Product.* 438:140583. DOI:10.1016/j.jclepro.2024.140583
37. Zhang W. and Li H. (2025). A study of the effect of motor structural components on harmonic noise. *Sci. Rep.* 15:7670. DOI:10.1038/s41598-025-91861-9
38. Wang F., Harindintwali J. D., Yuan Z., et al. (2021). Technologies and perspectives for achieving carbon neutrality. *The Innovation* 2:100180. DOI:10.1016/j.xinn.2021.100180
39. Yin Z., Zhou B., Duan M., et al. (2023). Climate extremes become increasingly fierce in China. *The Innovation* 4:100406. DOI:10.1016/j.xinn.2023.100406
40. Cohen J., Moeltner K., Reichl J., et al. (2018). Effect of global warming on willingness to pay for uninterrupted electricity supply in European nations. *Nat. Energy* 3:37–45. DOI:10.1038/s41560-017-0045-4
41. Salvo A. (2018). Electrical appliances moderate households' water demand response

to heat. *Nat. Commun.* **9**:5408. DOI:10.1038/s41467-018-07833-3
42. Woods J., James N., Kozubal E., et al. (2022). Humidity's impact on greenhouse gas emissions from air conditioning. *Joule* **6**:726–741. DOI:10.1016/j.joule.2022.02.013
43. Poredoš P., Shan H. and Wang R. (2022). Dehumidification with solid hygroscopic sorbents for low-carbon air conditioning. *Joule* **6**:1390–1393. DOI:10.1016/j.joule.2022.06.020
44. Ahmed F., Ramana A. S. and Jayakumar K. (2025). Experimental study on adiabatic pre-cooling systems for air cooled condensers in hot and humid climates. *Sci. Rep.* **15**:4933. DOI:10.1038/s41598-024-82863-0

FUNDING AND ACKNOWLEDGMENTS

The work described in this paper was sponsored by National Natural Science and Foundation of China (#52394223&52208011) . Any opinions, findings, conclusions, or recommendations expressed in this paper are those of the authors and do not necessarily reflect the views of those organizations.

AUTHOR CONTRIBUTIONS

All authors contributed to the manuscript and approved the final version.

DECLARATION OF INTERESTS

The authors declare no competing interests.

DATA AND CODE AVAILABILITY

Data are available from the corresponding author upon reasonable request.

SUPPLEMENTAL INFORMATION

It can be found online at: https://doi.org/10.59717/j.xinn-energy.2026.100136